ChemComm

COMMUNICATION

View Article Online
View Journal | View Issue

Cite this: *Chem. Commun.*, 2016, 52, 12466

Received 4th August 2016,
Accepted 20th September 2016

DOI: 10.1039/c6cc06432a

www.rsc.org/chemcomm

A supramolecular fluorescent vesicle based on a coordinating aggregation induced emission amphiphile: insight into the role of electrical charge in cancer cell division†

Jie Li,[a] Kangjie Shi,[a] Markus Drechsler,[b] Ben Zhong Tang,*[cd] Jianbin Huang*[a] and Yun Yan*[a]

Binding of Zn^{2+} to the coordinating supramolecular vesicle based on an aggregation induced emission amphiphile TPE-BPA immediately triggers the formation of charged vesicles. This induces vesicle fission and fluorescence reduction, suggesting a looser molecular packing in the charged vesicle membrane. Since cancer cells are highly charged, this indicates that the quick fission of cancer cells may have electrical charge origin.

Cancer cells are notorious for their quick reproduction and easy metastasis which cause serious threats to human lives.[1–6] To date, the code that governs the quick fission and metastasis of cancer has not been cracked, yet it is well-known that the membrane of cancer cells has much higher electrical charge[7–10] which is generally considered to be caused by the change of the membrane contents.[11] A recent study shows that alternating the electrical field may inhibit the metastatic spread of cancer.[12–15] However, so far the role of electrical charge in the fission of the membrane of cancer cells has not been clearly revealed, which is to a large extent due to the lack of a suitable modelling system.

Vesicles have long been considered as model systems for biological cells, yet so far studies in this regard have focused on the membrane behaviour of normal cells.[16–22] The corresponding studies on cancer cells are scarce, because most vesicles self-assembled from small molecules disassemble if the electrical charge of the component molecules increases,[23–26] whereas polymeric vesicles often exhibit "breathing" behaviour, namely, the size of the same vesicle increases upon increasing the electrical charge but contracts upon discharging.[27,28] It is highly desired to design robust vesicles that retain the vesicular structure at high electrical charge for the modelling of cancer cells.

Herein we report a case of a fluorescent vesicle built with the ionic supramolecular self-assembly of an aggregation induced emission (AIE)[29] amphiphile. This vesicle divides into many smaller ones when triggered by electrical charge, which is accompanied by the reduction of fluorescence, suggesting a looser molecular packing in the charged vesicles. The drug releasing test indicates that the releasing rate of the charged vesicle is 7 times that of the uncharged one. This model system, taking the advantage of the coordinating aggregation induced emission (AIE) molecule, for the first time reveals that electrical charge not only promotes the membrane division of cancer cells, but also leads to looser molecular packing in the cancer cells which facilitates much quicker mass exchange through the membrane.

The structure of TPE-BPA is given in Scheme 1a. Since each ligand carries 2 negative charges, TPE-BPA is highly soluble in water and emits weakly. However, upon addition of cationic surfactant CTAB (cetyltrimethylammonium bromide), intense emission can be induced, indicating that it is a typical AIE molecule.[29,30] The zeta potential of TPE-BPA in aqueous solution is −17 mV, but it increases sharply upon addition of cationic CTAB. A zero potential is obtained at a CTAB : TPE-BPA molar ratio of 8 : 1 (Fig. 1a), suggesting the formation of a neutral electrostatic complex TPE-BPA@8CTAB. In line with this, the fluorescence shows the maximum emission (Fig. 1b and c), and UV spectra display the largest red-shift (Fig. 1d), confirming the occurrence of the optimal interaction between TPE-BPA and CTAB at a molar ratio of 1 : 8.

The Cryo-TEM observation reveals that unilamellar and multilamellar vesicles (Fig. 2a and Fig. S1, ESI†) with an average size of ~145 nm have been formed, which is consistent with the result obtained from DLS measurements (Fig. 2b). The confocal laser scanning microscopy (CLSM) image indicates that these vesicles are fluorescent (inset in Fig. 2b), confirming the presence of TPE-BPA components in the vesicle membrane. The AFM image in Fig. S2 (ESI†) shows that the thickness of the

[a] *Beijing National Laboratory for Molecular Sciences, Institution College of Chemistry and Molecular Engineering, Peking University, Beijing, 100871, China. E-mail: yunyan@pku.edu.cn, jbhuang@pku.edu.cn*
[b] *University of Bayreuth, Bayreuth, D-95440, Germany*
[c] *Department of Chemistry, Division of Biomedical Engineering, The Hong Kong University of Science & Technology, Clear Water Bay, Kowloon, Hong Kong, China. E-mail: tangbz@pku.edu.cn*
[d] *Hong Kong Branch of Chinese National Engineering Research Center for Tissue Restoration and Reconstruction, Hong Kong, China*

† Electronic supplementary information (ESI) available. See DOI: 10.1039/c6cc06432a

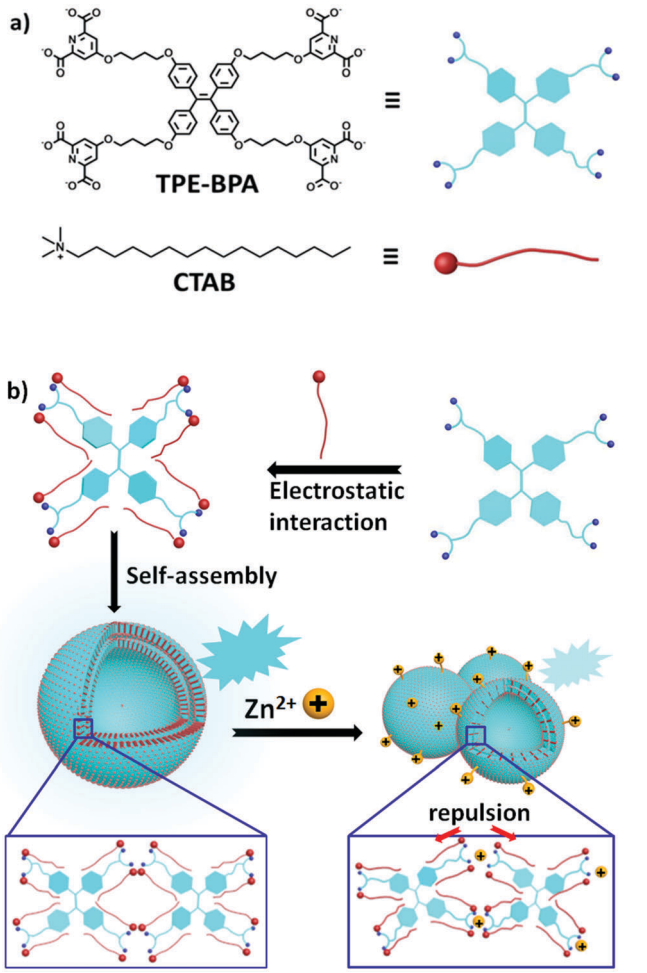

Scheme 1 (a) Molecular structures of TPE-BPA and CTAB. (b) Illustration of self-assembly of TPE-BPA/CTAB vesicles and electrical charge triggered fission of the TPE-BPA/CTAB vesicle.

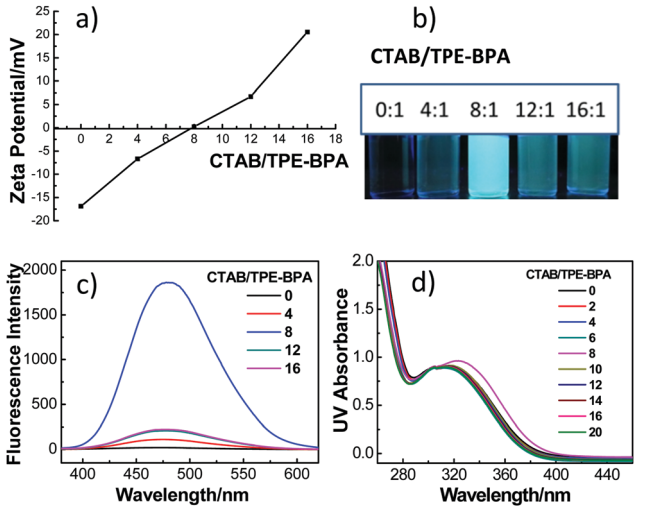

Fig. 1 (a) Variation of the zeta potential with different CTAB/TPE-BPA molar ratios; (b) photo of the CTAB/TPE-BPA samples under a 365 nm UV lamp at various molar ratios; (c) fluorescence spectra of the CTAB/TPE-BPA samples of different molar ratios; (d) UV spectra of the CTAB/TPE-BPA samples. [TPE-BPA] = 50 μM, T = 298 K. λ_{ex} = 365 nm.

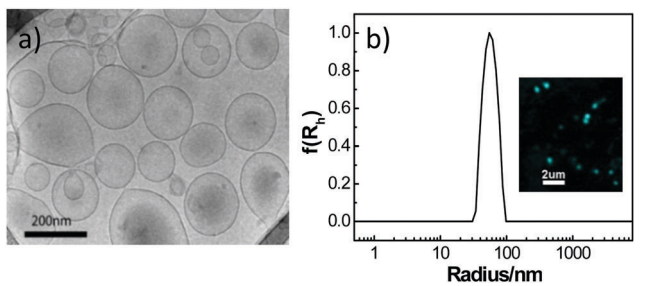

Fig. 2 Morphology and size information for the TPE-BPA@8CTAB vesicles: (a) cryo-TEM image; (b) size distribution obtained from DLS measurements. Inset in (b) is the CLSM image of the TPE-BPA@8CTAB vesicle.

collapsed vesicles can be 21.0 nm, 39.8 nm, *etc.* Since the extending length of TPE-BPA is about 2.5 nm and it always stretches in the membrane of the vesicle, the smallest height for a dry vesicle should be equal to the sum of two collapsed TPE-BPA layers, namely, about 5.0 nm. Therefore, heights of 21.0 and 39.8 nm correspond to multilamellar vesicles with 4 and 8 shells, respectively. Obviously, the vesicle membrane is formulated by the TPE-BPA monolayer, and CTAB, with an extending length of 1.5 nm, has to embed into the voids between the coordinating heads of TPE-BPA (Scheme 1b). Since TPE-BPA on its own cannot self-assemble, we expect that the increased hydrophobic effect in the TPE-BPA@8CTAB supramolecular building block is the main driving force for the formation of vesicles.

As the hydrophilic heads of TPE-BPA molecules are capable of coordinating with metal ions, such as Zn^{2+},[31] Ni^{2+},[32] Ca^{2+},[32] *etc.*, Zn^{2+} is added to the TPE-BPA@8CTAB vesicular system. (Zn^{2+} has no quenching effect on the luminescence of TPE group.[32]) Fig. 3a shows that fluorescence keeps decreasing upon addition of Zn^{2+} and reaches a plateau at a Zn^{2+}/TPE-BPA ratio of 2. Meanwhile, the UV absorption at 255 nm keeps increasing and levels off at this ratio (Fig. 3b). Since each TPE-BPA contains 4 coordinating heads (pyridine dicarboxylate ligands), and in principle each Zn^{2+} can coordinate with two pyridine dicarboxylate ligands,[31,33] this implies that every two coordinating heads share one Zn^{2+} to satisfy the space of an octahedral field,[34,35] as illustrated in Fig. S3 (ESI†). Therefore, we propose that the neighbouring two pyridine dicarboxylate ligands coordinate to the same Zn^{2+}, as illustrated in Scheme 1b.

DLS measurements (Fig. S4a, ESI†) suggest that smaller particles with a hydrodynamic diameter of about 35 nm are formed upon addition of Zn^{2+} to the TPE-BPA@8CTAB vesicular system. Number averaged analysis indicates that the small particles are the dominant species (Fig. S4b, ESI†). The Cryo-TEM observation reveals that the smaller particles still retain the vesicular structure (Fig. 3b, inset), which is further confirmed in the AFM measurement (Fig. 3c). The height profiles indicate that the collapsed particles are about 10.5 nm and 5.1 nm (Fig. 3c). These values are much smaller than 35 nm, suggesting that these particles are hollow vesicles. It is worth noting that the scattering intensity (Fig. 3d) for the small vesicles is

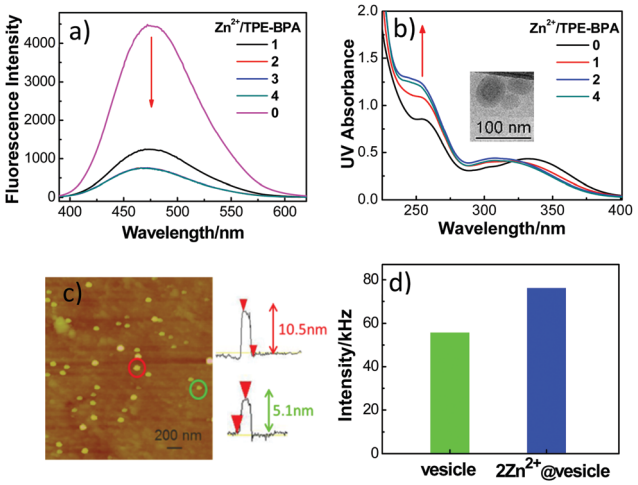

Fig. 3 (a) Variation of the fluorescence, (b) UV/Vis absorption with the addition of Zn^{2+} to the TPE-BPA@8CTAB vesicular system; (c) AFM image and the height profile of the $2Zn^{2+}$@TPE-BPA@8CTAB vesicles; (d) scattered intensity of the TPE-BPA@8CTAB vesicular system before and after addition of Zn^{2+}. [TPE-BPA] = 50 μM, [CTAB] = 400 μM, [Zn^{2+}] = 100 μM. Inset in (b) is the cryo-TEM image of the $2Zn^{2+}$@TPE-BPA@8CTAB vesicles.

about 25% higher than that of the larger ones. Since the scattering intensity is proportional to R^6, where R is the radius of the scattering particle, the observation of increased scattered light intensity strongly indicates that the number of small particles is tremendous. Therefore, it is convinced that Zn^{2+} ions have triggered the fission of the TPE-BPA@8CTAB vesicles (Scheme 1b).

The Zn^{2+} triggered vesicle fission is attributed to the increased surface charge. Fig. 4a demonstrates that after addition of Zn^{2+} ions, the zeta potential of the vesicles keeps increasing and reaches a plateau at an optimal coordinating Zn^{2+}/TPE-BPA ratio of 2. In a controlled experiment where Zn^{2+} is replaced with Ca^{2+}, a cation displaying much weaker binding affinity to the head of TPE-BPA,[36] the zeta potential of the vesicles only slightly increases (Fig. 4a). In line with this, the size of the vesicles is hardly influenced (Fig. 4b). Accordingly, the fluorescence intensity and UV absorbance (Fig. S5, ESI†) are not influenced, too.

The electrical charge triggered vesicle fission can be qualitatively explained using the theory of molecular packing,[37,38] where the packing parameter P is expressed as $P = v/al$, with v, a, and l being the volume of the hydrophobic part, the average occupied

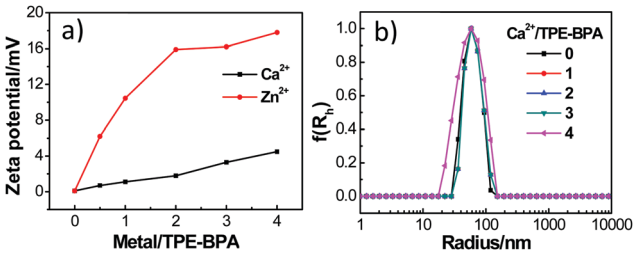

Fig. 4 (a) Comparison of the zeta potential of the TPE-BPA@8CTAB vesicle triggered by Zn^{2+} and Ca^{2+}. (b) DLS size distribution of the TPE-BPA@8CTAB vesicle in the presence of various amounts of Ca^{2+}.

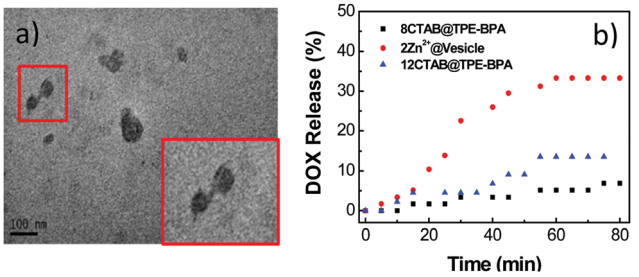

Fig. 5 (a) TEM image of the fission of the TPE-BPA@8CTAB vesicle triggered by Zn^{2+}. The image was captured after addition of Zn^{2+} within 1 minute. [TPE-BPA] = 50 μM, [CTAB] = 400 μM, [Zn^{2+}] = 100 μM. Inset in (a) is the TEM image of the vesicles in the process of fission with high magnification. (b) Comparison of the DOX releasing rate in the native TPE-BPA@8CTAB vesicle and the charged vesicle of the TPE-BPA@12CTAB, $2Zn^{2+}$@vesicle. [TPE-BPA] = 50 μM, [CTAB] = 400 μM, [Zn^{2+}] = 100 μM, [DOX] = 100 μM, T = 25 °C.

area of the component molecule, and the extending length of the hydrophobic chains, respectively. P increases as the self-assembled structure develops from micelles (P = 0–1/3) to vesicles (P = 1/2–1). Generally speaking, in the reasonable P range, larger P will lead to the formation of larger particles. As the surface charge of the vesicles is increased, repulsive forces between molecules in the membrane are generated, which lead to a larger occupied area per molecule. As a result, the value of P is decreased, so that smaller vesicles are formed.

It is worth noting that the electrical charge triggered fission of vesicles is not the same as that of the 'breathing' vesicles reported in the literature,[27,28] where increasing electrical charge does not change the number of vesicles but generate a larger one as a result of repulsion inside the same vesicle. In contrast, in the present study, the increased charge has resulted in an increased number of vesicles but decreased size. Fig. 5a clearly shows that after addition of Zn^{2+} ions for 1 min, the vesicles become ellipsoid, and divide into several smaller ones.

Since the membranes of cancer cells are highly charged compared to the normal ones,[7–10] the present results indicate that the high electrical charge may accelerate the cell fission and generate a looser molecular packing. Because TPE-BPA is a typical AIE molecule which displays emission proportional to the extent of aggregation,[39] the decrease of the emission is a reflection of the looser molecular packing. To confirm this argument further, the releasing rates displayed by vesicles with different charges were compared. Fig. 5b shows that when a hydrophilic drug DOX is entrapped in the native charge neutral vesicle of TPE-BPA@8CTAB, only 5% of the drug is released within 60 min. In contrast, as the charges are increased upon increasing the composition of CTAB to form the TPE-BPA@12CTAB vesicle (ζ = 6.4 mV), the releasing rate is enhanced to 15% within 60 min. Not surprisingly, nearly 35% of DOX is released from the $2Zn^{2+}$@vesicle within the same time scale since it has a much higher potential of ζ = 16.5 mV. The charge dependent releasing rate demonstrates that the molecular exchange through the membrane has been significantly promoted in the charged vesicle. We expect that this may facilitate the metastatic spread of cancer factors.

In summary, we for the first time report the triggered fission of vesicles with increasing electrical charge. The vesicle is built with the supramolecular vesicle of ionic self-assembly of a coordinating aggregation induced emission amphiphile. The original low charged strong luminescent vesicle immediately undergoes fission upon coordination with Zn^{2+}, which is accompanied by the drastic increase of the surface electrical potential and the decrease of the fluorescence, indicating a much looser molecular packing in the highly charged vesicles. The drug releasing experiment reveals a faster molecular exchange through the charged vesicular membrane, which confirms the occurrence of looser molecular packing. Because a prominent feature of cancer cells is their abnormally high surface charge potential, this model system clearly indicates that the electrical charges are very relevant to the fission and molecular arrangement in the membrane of cancer cells, which may help to reveal the mystery behind the easy metastasis of the cancer cells and inspire a novel strategy for cancer therapy.

This work is supported by the National Science Foundation of China (NSFC, Grant No. 21422302, 21573011, and 21173011), National Basic Research Program of China (2013CB933800), and the Innovation and Technology Commission of Hong Kong (ITC-CNERC14S01).

Notes and references

1 L. A. Torre, F. Bray, R. L. Siegel, J. Ferlay, J. Lortet-Tieulent and A. Jemal, *Ca-Cancer J. Clin.*, 2015, **65**, 87–108.
2 T. L. Whiteside, *Oncogene*, 2008, **27**, 5904–5912.
3 S. Valastyan and R. A. Weinberg, *Cell*, 2011, **147**, 275–292.
4 J. Ferlay, I. Soerjomataram, R. Dikshit, S. Eser, C. Mathers, M. Rebelo, D. M. Parkin, D. Forman and F. Bray, *Int. J. Cancer*, 2015, **136**, 359–386.
5 L. Wan, K. Pantel and Y. Kang, *Nat. Med.*, 2013, **19**, 1450–1464.
6 C. L. Chaffer and R. A. Weinberg, *Science*, 2011, **331**, 1559–1564.
7 E. C. Cho, J. Xie, P. A. Wurm and Y. Xia, *Nano Lett.*, 2009, **9**, 1080–1084.
8 E. J. Ambrose, A. M. James and J. H. B. Lowick, *Nature*, 1956, **177**, 576–577.
9 I. Dobrzyńska, B. Szachowicz-Petelska, S. Sulkowski and Z. Figaszewski, *Mol. Cell. Biochem.*, 2005, **276**, 113–119.
10 N. M. Goldenberg and B. E. Steinberg, *Cancer Res.*, 2010, **70**, 1277–1280.
11 T. Yeung, G. E. Gilbert, J. Shi, J. Silvius, A. Kapus and S. Grinstein, *Science*, 2008, **319**, 210–213.
12 E. D. Kirson, V. Dbalý, F. Tovaryš, J. Vymazal, J. F. Soustiel, A. Itzhaki, D. Mordechovich, S. Steinberg-Shapira, Z. Gurvich and R. Schneiderman, *Proc. Natl. Acad. Sci. U. S. A.*, 2007, **104**, 10152–10157.
13 E. D. Kirson, M. Giladi, Z. Gurvich, A. Itzhaki, D. Mordechovich, R. S. Schneiderman, Y. Wasserman, B. Ryffel, D. Goldsher and Y. Palti, *Clin. Exp. Metastasis*, 2009, **26**, 633–640.
14 B. Szachowicz-Petelska, I. Dobrzyńska, Z. Figaszewski and S. Sulkowski, *Mol. Cell. Biochem.*, 2002, **238**, 41–47.
15 M. Linnert, B. Agerholm-Larsen, F. Mahmood, H. K. Iversen and J. Gehl, *Tumors of the Central Nervous System*, Springer, 2014, vol. 12, pp. 247–259.
16 T. Hamada, H. Hagihara, M. Morita, M. D. C. Vestergaard, Y. Tsujino and M. Takagi, *J. Phys. Chem. Lett.*, 2012, **3**, 430–435.
17 M. Andes-Koback and C. D. Keating, *J. Am. Chem. Soc.*, 2011, **133**, 9545–9555.
18 A.-S. Cans, N. Wittenberg, R. Karlsson, L. Sombers, M. Karlsson, O. Orwar and A. Ewing, *Proc. Natl. Acad. Sci. U. S. A.*, 2003, **100**, 400–404.
19 J. Zimmerberg, F. Cohen and A. Finkelstein, *Science*, 1980, **210**, 906–908.
20 F. M. Menger and M. I. Angelova, *Acc. Chem. Res.*, 1998, **31**, 789–797.
21 W. Jiang, Y. Zhou and D. Yan, *Chem. Soc. Rev.*, 2015, **44**, 3874–3889.
22 U. J. Meierhenrich, J.-J. Filippi, C. Meinert, P. Vierling and J. P. Dworkin, *Angew. Chem., Int. Ed.*, 2010, **49**, 3738–3750.
23 Q. He, Y.-F. Ao, Z.-T. Huang and D.-X. Wang, *Angew. Chem., Int. Ed.*, 2015, **54**, 11785–11790.
24 Q. Yan, J. Yuan, Z. Cai, Y. Xin, Y. Kang and Y. Yin, *J. Am. Chem. Soc.*, 2010, **132**, 9268–9270.
25 D.-S. Guo, K. Wang, Y.-X. Wang and Y. Liu, *J. Am. Chem. Soc.*, 2012, **134**, 10244–10250.
26 G. Yu, X. Zhou, Z. Zhang, C. Han, Z. Mao, C. Gao and F. Huang, *J. Am. Chem. Soc.*, 2012, **134**, 19489–19497.
27 S. Y. Yu, T. Azzam, I. Rouiller and A. Eisenberg, *J. Am. Chem. Soc.*, 2009, **131**, 10557–10566.
28 R. J. Dong, B. S. Zhu, Y. F. Zhou, D. Y. Yan and X. Y. Zhu, *Angew. Chem., Int. Ed.*, 2012, **51**, 11633–11637.
29 J. D. Luo, Z. L. Xie, J. W. Y. Lam, L. Cheng, H. Y. Chen, C. F. Qiu, H. S. Kwok, X. W. Zhan, Y. Q. Liu, D. B. Zhu and B. Z. Tang, *Chem. Commun.*, 2001, 1740–1741.
30 Y. Hong, J. W. Y. Lam and B. Z. Tang, *Chem. Soc. Rev.*, 2011, **40**, 5361–5388.
31 Y. Yan, N. A. M. Besseling, A. de Keizer, A. T. M. Marcelis, M. Drechsler and M. A. C. Stuart, *Angew. Chem., Int. Ed.*, 2007, **46**, 1807–1809.
32 L. M. Xu, L. X. Jiang, M. Drechsler, Y. Sun, Z. R. Liu, J. B. Huang, B. Z. Tang, Z. B. Li, M. A. C. Stuart and Y. Yan, *J. Am. Chem. Soc.*, 2014, **136**, 1942–1947.
33 Y. Yan, A. A. Martens, N. A. M. Besseling, F. A. de Wolf, A. de Keizer, M. Drechsler and M. A. C. Stuart, *Angew. Chem., Int. Ed.*, 2008, **47**, 4192–4195.
34 J. C. MacDonald, P. C. Dorrestein, M. M. Pilley, M. M. Foote, J. L. Lundburg, R. W. Henning, A. J. Schultz and J. L. Manson, *J. Am. Chem. Soc.*, 2000, **122**, 11692–11702.
35 M. V. Yigit, K. Biyikli, B. Moulton and J. C. MacDonald, *Cryst. Growth Des.*, 2006, **6**, 63–69.
36 E. Norkus, I. Stalnionienė and D. C. Crans, *Heteroat. Chem.*, 2003, **14**, 625–632.
37 W. Kunz, F. Testard and T. Zemb, *Langmuir*, 2009, **25**, 112–115.
38 Y. Yan, W. Xiong, X. Li, T. Lu, J. Huang, Z. Li and H. Fu, *J. Phys. Chem. B*, 2007, **111**, 2225–2230.
39 C. S. Zhu, S. P. Pang, J. P. Xu, L. Jia, F. M. Xu, J. Mei, A. J. Qin, J. Z. Sun, J. Ji and B. Z. Tang, *Analyst*, 2011, **136**, 3343–3348.